Leading-order hadronic contributions to the lepton anomalous magnetic moments from the lattice

Florian Burger[1], Xu Feng[2], Karl Jansen[4], Marcus Petschlies[5,a], Grit Pientka[3], and Dru B. Renner[6]

[1]*OakLabs GmbH, Neuendorfstr. 20B, D-16761 Hennigsdorf, Germany*

[2]*Columbia University, Department of Physics, 538 West 120th Street, 704 Pupin Hall, New York, NY 10027, USA*

[3]*Humboldt-Universität zu Berlin, Institut für Physik, Newtonstr. 15, D-12489 Berlin, Germany*

[4]*NIC, DESY, Platanenallee 6, D-15738 Zeuthen, Germany*

[5]*Rheinische Friedrich-Wilhelms-Universität Bonn, Institut für Strahlen- und Kernphysik, Nußallee 14-16, D-53115 Bonn, Germany*

[6]*Los Alamos National Laboratory (LANL), P.O. Box 1663, Los Alamos, NM 87545, USA*

Abstract. The hadronic leading-order (hlo) contribution to the lepton anomalous magnetic moments a_l^{hlo} of the Standard Model leptons still accounts for the dominant source of the uncertainty of the Standard Model estimates. We present the results of an investigation of the hadronic leading order anomalous magnetic moments of the electron, muon and tau lepton from first principles in twisted mass lattice QCD. With lattice data for multiple pion masses in the range $230\,\text{MeV} \lesssim m_{PS} \lesssim 490\,\text{MeV}$, multiple lattice volumes and three lattice spacings we perform the extrapolation to the continuum and to the physical pion mass and check for all systematic uncertainties in the lattice calculation. As a result we calculate a_l^{hlo} for the three Standard Model leptons with controlled statistical and systematic error in agreement with phenomenological determinations using dispersion relations and experimental data. In addition, we also give a first estimate of the hadronic leading order anomalous magnetic moments from simulations directly at the physical value of the pion mass.

1 Introduction

Lattice QCD offers the opportunity to study hadronic contributions to electroweak observables from first principles. This conference contribution focuses on the hadronic leading order (in the electroweak couplings) contribution to the anomalous magnetic moments a_l^{hlo} of the Standard Model leptons electron, muon and tau. Beyond these important quantities the calculation shown here can be adapted to a broad range of applications for a variety of quantities such as the next-to-leading order vacuum-polarization type contributions to the lepton anomalous magnetic moments, the hadronic running of the electroweak couplings α_{QED} and $\sin^2(\theta)$, the Adler function or Λ_{QCD} amongst others [25].

As a crucial prerequisite, the nonperturbative hadron dynamics entering all these quantities can be calculated entirely in Euclidean spacetime. This makes them accessible to ab-initio lattice calculations, which simulate the strong interaction of quarks and gluons on a Euclidean spacetime lattice. For the muon anomalous magnetic moment in particular, this has been worked out in the pioneering work by Blum [1]. On the other hand, the regularization of QCD by the finite lattice volume L^3, the lattice spacing a and the simulation at unphysically large pion masses introduce a systematic dependence on the infrared and ultraviolet cutoff, $1/L$ and $1/a$, respectively, and the

light pseudoscalar mass, which need to be extrapolated with care to the corresponding limits, $L \to \infty$, $a \to 0$ and $m_{PS} \to m_\pi$.

The simulation effort by the European Twisted Mass Collaboration (ETMC) has matured to a state, at which we can calculate the above mentioned quantities for multiple lattice volumes, lattice spacings and pion masses close to or even at the physical point with contributions from up, down, strange and charm quarks. Within this framework we are now able to reach for high-precision results from lattice QCD with control over systematic uncertainties. In this contribution we report our progress for the hadronic leading order contribution to the anomalous magnetic moments of the Standard Model leptons towards the goal of reaching the current precision obtained in phenomenological analyses using experimental data.

The essential ingredient for this calculation is the hadronic vacuum polarization tensor and function

$$\Pi_{\mu\nu}^{AB}(Q) = \int d^4x \, \langle J_\mu^A(x) J_\nu^B(y) \rangle \, e^{iQ(x-y)}$$
$$= \left(Q_\mu Q_\nu - \delta_{\mu\nu} Q^2 \right) \Pi^{AB}(Q^2). \quad (1)$$

determined from lattice QCD. Here J_μ^A denotes a flavor diagonal isospin component of the vector current or a linear combination of such components. In particular a_l^{hlo} requires the vacuum polarization function from the 2-point correlator of electromagnetic currents, $A = \gamma$, as part of

the integrand for the QED-1-loop integral (cf. figure [1]) [1]

$$a_l^{\text{hlo}} = 4\,\alpha^2 \int \frac{dQ^2}{Q^2}\, \Pi_R^{\gamma\gamma}(Q^2)\, w\left(Q^2/m_l^2\right). \qquad (2)$$

with the subtracted vacuum polarization function

$$\Pi_R^{\gamma\gamma}(Q^2) = \Pi^{\gamma\gamma}(Q^2) - \Pi^{\gamma\gamma}(0).$$
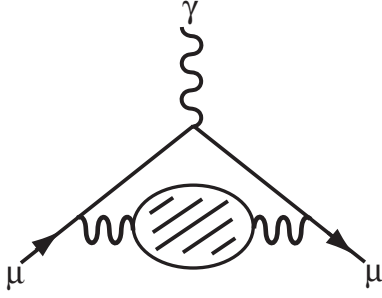

Figure 1. Hadronic leading order correction to the muon-photon-vertex

The muon anomalous magnetic moment has been determined both experimentally and theoretically to an uncertainty of approximately 0.5 ppm with a discrepancy of 2 to 4 standard deviations between the experimental and the Standard Model value [3]

$$a_\mu(\text{EXP}) = 11659208.9\,(6.3) \cdot 10^{-10},$$
$$a_\mu(\text{SM}) = 11659180.4\,(4.2)\,(2.6) \cdot 10^{-10}.$$

$a_\mu(\text{SM})$ is not a pure Standard Model number, though, since its extraction partly relies on experimental data and some amount of modeling. It has thus become a focal point of numerous studies in lattice QCD with an enhanced effort to investigate the systematic uncertainties which arise naturally in the framework of a lattice QCD calculation, such as the finite lattice volume.

Though not immediately apparent from the definition in equation (2), the extension of the lattice QCD calculation to the electron and tau hadronic leading order anomalous magnetic moments is a non-trivial step. From the practical point of view the calculation is universal for all three leptons, since the specific lepton property only enters via the lepton mass in the analytically known weight function $w\left(Q^2/m_l^2\right)$ in the integrand. But the ratios of the lepton masses $m_e^2 : m_\mu^2 : m_\tau^2 \approx 1 : 4 \cdot 10^4 : 10^7$ extending over 7 orders of magnitude imply a significantly different weighting of the momentum dependence of the polarization function in the momentum integration for the individual leptons. As a consequence the individual lattice artifacts will have significantly different bearings on a_l^{hlo}, in each case, which we discuss in more detail below.

2 Twisted mass lattice QCD calculation

We use the twisted-mass lattice regularization of QCD [9] for a mass degenerate light quark doublet $\chi_l = (u,d)^T$

and a non-degenerate heavy quark doublet $\chi_h = (c,s)^T$ together with the Iwasaki gauge action [22]. The sea-quark action is given by

$$S_{\text{sea}} = \sum_x \bar{\chi}_l(x)\left(D_W + i\mu_l\,\gamma_5\,\tau^3\right)\chi_l(x)$$
$$+ \sum_x \bar{\chi}_h(x)\left(D_W + i\mu_\sigma\,\gamma_5\,\tau^1 + \mu_\delta\,\tau^3\right)\chi_h(x). \quad (3)$$

D_W is the Wilson-Dirac operator

$$D_W = \frac{1}{2}\,\gamma_\mu\left(\nabla_\mu^f + \nabla_\mu^b\right) - \left(\frac{ar}{2}\,\nabla_\mu^b\,\nabla_\mu^f - m_{\text{cr}}\right) + (m_0 + m_{\text{cr}}) \qquad (4)$$

where ∇^f, ∇^b denote the gauge-covariant, discrete forward and backward derivative, m_0 the bare quark mass and $\tau^{1,2,3}$ the Pauli matrices. The twisted mass term for the heavy quark doublet $i\gamma_5\,\tau^1\,\mu_\sigma$ breaks the vector part of isospin symmetry such that the flavor diagonal isovector currents, and in particular also the electromagnetic current, are no longer conserved. We thus use a mixed action ansatz with a valence quark action, that has improved isospin symmetry [8, 10, 19],

$$S_{\text{val}} = \sum_{f=l,s,c}\sum_x \bar{\psi}_f(x)\left(D_W + i\mu_f\,\gamma_5\,\tau^3\right)\psi_f(x) \quad (5)$$

$$\psi_f = \left(\psi_f^+,\,\psi_f^-\right)^T. \qquad (6)$$

Using this mixed action on the lattice has been shown to guarantee the automatic absence of lattice artifacts of $O(a)$ in the continuum limit of physical, on-shell observables [10] by solely tuning the bare quark mass m_0 to its critical value $m_0 \to m_{\text{cr}}$ without any further improvement of lattice action or operators. This property remains true for the hadronic vacuum polarization function $\Pi^{\gamma\gamma}$ in the presence of off-shell, short distance contributions in equation (1) [20]. The renormalized strange and charm valence quark masses in the mixed action are fixed by requiring $2m_K^2 - m_{PS}^2$ and the D-meson mass calculated in the valence sector to attain their physical value.

The gauge field ensembles with $N_f = 2 + 1 + 1$ dynamical quarks produced by the ETMC and used for this calculation are listed in table {1}. Details about their production and properties are given in references [6, 7]. Additionally, we consider one ETMC ensemble at the physical pion mass [16, 17, 21], whose parameters are listed in the last row of the table.

For the valence quark action eq. (5) the electromagnetic current on the lattice follows as the Noether current from the vector flavor variation

$$\delta\psi(x) = iQ^{\text{em}}\psi(x), \quad \delta\bar{\psi}(x) = -i\bar{\psi}(x)\,Q^{\text{em}} \qquad (7)$$

generated by the electromagnetic charge matrix $Q^{\text{em}} = \text{diag}\,(+2/3, -1/3, \ldots)$ acting in flavor space. Eq. (7) defines the electromagnetic current as the usual sum of single-flavor quark currents

$$J_\mu^\gamma = \frac{2}{3}\,J_\mu^u - \frac{1}{3}\,J_\mu^d + \frac{2}{3}\,J_\mu^c - \frac{1}{3}\,J_\mu^s$$

Table 1. Gauge field ensembles generated by the European Twisted Mass Collaboration with $N_f = 2 + 1 + 1$ dynamical quarks [6, 7] and with $N_f = 2$ dynamical quark flavors at physical pion mass [16, 17] (last row).

Ensemble	a[fm]	m_{PS} [MeV]	L[fm]	$m_{PS} \cdot L$
D15.48	0.061	227	2.9	3.3
D30.48	0.061	318	2.9	4.7
D45.32sc	0.061	387	1.9	3.7
B25.32t	0.078	274	2.5	3.5
B35.32	0.078	319	2.5	4.0
B35.48	0.078	314	3.7	5.9
B55.32	0.078	393	2.5	5.0
B75.32	0.078	456	2.5	5.8
B85.24	0.078	491	1.9	4.7
A30.32	0.086	283	2.8	4.0
A40.32	0.086	323	2.8	4.6
A50.32	0.086	361	2.8	5.1
cA2.09.48	0.091	$\approx m_\pi$	4.4	3.0

Figure 2. Diagrammatic representation of the quark-connected (left) and (exemplary) quark-disconnected contribution to the vacuum polarization; black lines denote valence quark loops and gray shading represents full, non-perturbative QCD interaction.

and the lattice vacuum polarization tensor

$$\Pi_{\mu\nu}^{\gamma\gamma}(x, y) = \langle J_\mu^\gamma(x) \, J_\nu^\gamma(y) \rangle - a^{-3} \, \delta_{x,y} \, \delta_{\mu\nu} \, \langle S_\nu(y) \rangle \quad (8)$$

as the 2-point current correlator with a lattice contact term. The tensor fulfills the lattice version of exact transversality at non-zero lattice spacing

$$\partial_\mu^b \, \Pi_{\mu\nu}^{\gamma\gamma}(x, y) = 0 \quad (9)$$

with the discrete backward partial derivative ∂_μ^b.

The discrete 4-dimensional Fourier transform translates this transversality to momentum space

$$\Pi_{\mu\nu}(Q) = \sum_x \Pi_{\mu\nu}(x, y) \, e^{iQ(x+a\hat{\mu}/2-y-a\hat{\nu}/2)}$$

$$\hat{Q}_\mu \, \Pi_{\mu\nu}(Q) = 0, \quad \hat{Q}_\mu = \frac{2}{a} \sin\left(aQ_\mu/2\right)$$

with $Q_i \in 2\pi/L \cdot \{0, \ldots, L/a - 1\}$ and $Q_0 \in 2\pi/T \cdot \{0, \ldots, T/a - 1\}$ for the spatial and temporal momentum components. We extract the polarization function according to

$$\Pi^{\gamma\gamma}\left(\hat{Q}^2\right) = \frac{1}{\# \left[\hat{Q}^2\right]} \sum_{Q \in [\hat{Q}^2]} \text{Re}\left(\sum_{\mu,\nu} P_{\mu\nu}(Q) \, \Pi_{\mu\nu}^{\gamma\gamma}(Q)\right)$$

$$\times \left(\sum_{\mu,\nu} P_{\mu\nu}(Q) \, P_{\mu\nu}(Q)\right)^{-1}, \quad (10)$$

$$P_{\mu\nu}(Q) = \hat{Q}_\mu \, \hat{Q}_\nu - \delta_{\mu\nu} \, \hat{Q}^2 .$$

The definition in eq. (10) includes the projection with $P_{\mu\nu}$, which is non-trivial for the index ν, and discarding the imaginary part, which is a lattice artifact due to flavor symmetry breaking. With a $\left[\hat{Q}^2\right]$ we denote the set of all lattice momenta Q with the same $\hat{Q}^2$ and with $\# \left[\hat{Q}^2\right]$ the number of such momenta.

The vacuum polarization tensor and function decompose into a dominant quark-connected and a small quark-disconnected contribution, which are illustrated by the left-hand and right-hand diagram in figure [2], respectively.
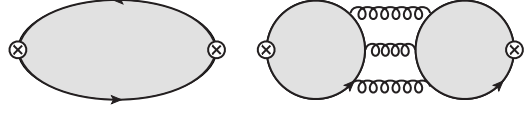
For illustration we show exemplary data for the connected and disconnected contribution to the vacuum polarization function in the left and right panel of figure [3], respectively. The left-hand panel shows the typical smooth momentum dependence of the connected contribution from up and down quarks for ensemble B25.32t (cf. table {1}) between the infrared and ultraviolet lattice cut-off $(2 \sin(a\pi/T)/a)^2 \leq \hat{Q}^2 \leq 16/a^2$. The gray band in the plot shows our standard fit to the data, which will be discussed below. In the detail plot we magnify the crucial region at small momenta, where lattice data points become sparse. The right-hand panel shows an order-of-magnitude comparison of the signal for the light-quark connected polarization function (blue band) and the disconnected contribution from the 2-point correlation of the isovector components of the electromagnetic current (dark-red band labeled isospin 1) and of the isoscalar components (yellow band labeled isospin 0). The data shown was obtained with particularly high statistics for ensemble B55.32, cf. [29]. While the contribution from the isovector currents is a lattice artifact in the twisted mass regularization, the physically meaningful contribution from the isoscalar vector current correlator appears about two orders of magnitude smaller compared to the connected contribution. In fact, with the presently available data we cannot resolve a statistically significant contribution from the disconnected vacuum polarization function to a_l^{hlo}. In the following we will thus be concerned only with the connected vacuum polarization function.

Momentum dependence of the polarization function

The lattice calculation generically provides us with data points for the vacuum polarization function for a finite set of discrete, nonzero momenta. According to equation (2) the subtracted polarization function enters the integrand and the integral extends beneath the lowest non-zero lattice momentum to zero. We thus need to extrapolate the existing lattice data to all $Q^2 < Q_{\text{min}}^2 = 4/a^2 \sin^2(\pi/L)$. Secondly, the infinite upper integration limit is relaxed to the lattice cut-off $Q_{\text{max}}^2 = 16/a^2$. To appreciate the significance of these two issues we display the integral saturation in the left-hand panel of figure [4]: shown is the ratio

$$R_l\left(Q_{\text{max}}^2\right) = \frac{a_l^{\text{hlo}}\left(Q_{\text{max}}^2\right)}{a_l^{\text{hlo}}\left(100\,\text{GeV}^2\right)} .$$
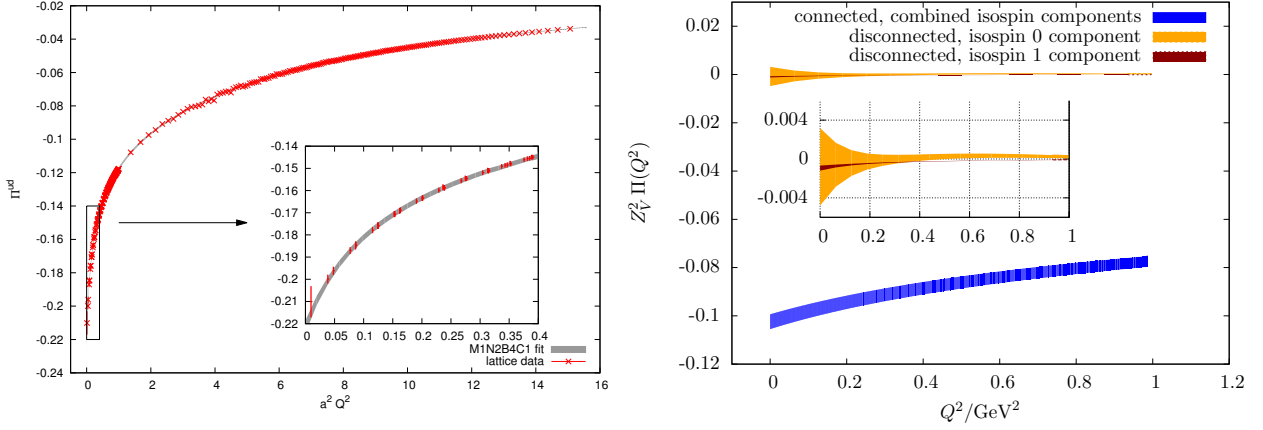
Figure 3. Left: quark-connected contribution from up and down quark to the hadronic vacuum polarization function; the data shown belongs to ensemble B25.32t (m_{PS} = 274 MeV, L = 2.5 fm and a = 0.078 fm). Right: quark-disconnected contribution from up and down quark for ensemble B55.32 (m_{PS} = 393 MeV, L = 2.5 fm and a = 0.078 fm).The detail plots show a magnification of the small-momentum region.
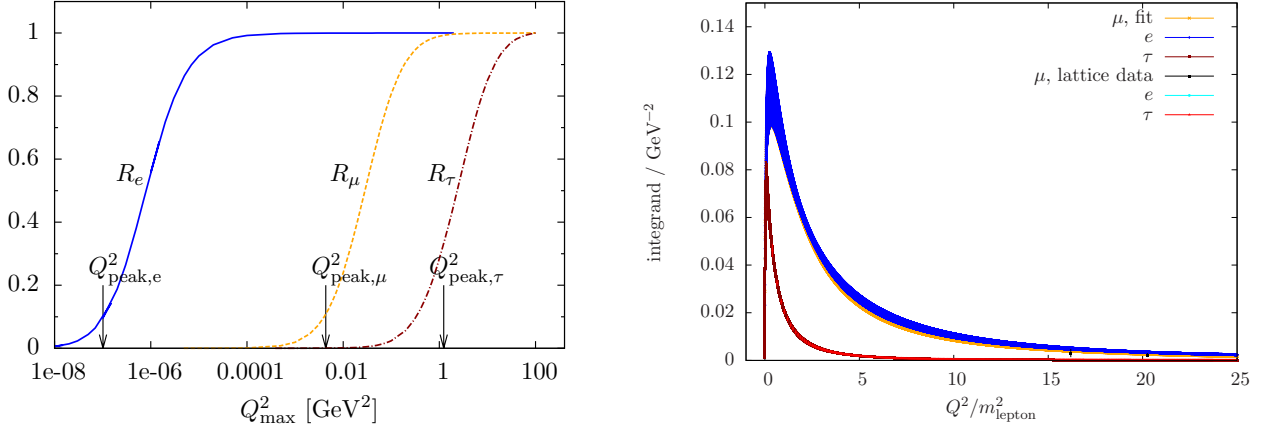

Figure 4. Left: saturation of the integral defining a_l^{hlo} for $l = e, \mu, \tau$; the data shown corresponds to ensemble B55.32. Right: the full integrand for ensemble D15.48 in a universal plot for all three leptons.

of a_l^{hlo} integrated from zero up to Q_{max}^l over the a_l^{hlo} integrated from zero up to $100\,\text{GeV}^2$. The plot shows, that the upper integration limit Q_{max}^2 on the lattice is not problematic, since for electron and muon the integral saturates long before reaching the lattice momentum cut-off and also for the tau the change of the integral value with $Q_{\text{max}}^2 \lesssim 100\,\text{GeV}^2$ is insignificant compared to the statistical and other sources of systematic uncertainties.

In the same plot $Q_{\text{peak},l}^2$ marks the maximum of the weight function $w\left(Q^2/m_l^2\right)$ for each lepton, which roughly locates the main support area for the integral. As is well known, for the electron and the muon this main support region is far below the lowest reachable lattice momentum for currently available lattice volumes. In particular $Q_{\text{min}}^2 \gtrsim 0.1\,\text{GeV}^2$ for our ensembles in table {1}. In the extreme case of the electron, a_l^{hlo} is essentially determined by the $d\Pi^{\gamma\gamma}/dQ^2(0)$ alone. The right panel in figure [4] shows the location of lattice data in comparison to the fitted integrand exemplarily for ensemble D15.48. While for the electron all lattice data is outside the displayed momentum range, for the muon the (black) lattice data points start at $Q^2/m_\mu^2 \approx 16$. For the tau (red) lattice data stops short of the peak on the right-hand slope of the integrand (brown band).

To fit the momentum dependence of the polarization function numerous fit ansätze can be constructed based on the analyticity and spectral properties of the polarization function, resonances and other features. In particular fit functions of the Padé type have been shown to be a suitable set [11, 23, 24] of functions with correct convergence properties to reproduce the analytic structure of $\Pi^{\gamma\gamma}$ in the limit of infinite volume and data precision. We here use the *MNBC* fit ansatz, which is conceptually close to the Padé type fits. Since at this point we consider only the connected part of $\Pi^{\gamma\gamma}$ we can decompose it immediately into single-quark-flavor components

$$\Pi^{\gamma\gamma} = \frac{5}{9}\Pi^{u+d} + \frac{1}{9}\Pi^s + \frac{4}{9}\Pi^c.$$

Further on, we decompose the integration interval in two regions: low momentum $0 \leq Q^2 \leq Q^2_{\text{match}}$ and high momentum $Q^2_{\text{match}} < Q^2 \leq Q^2_{\text{max}}$. Then for each individual quark flavor $f = u + d, s, c$ we use the family of fit functions

$$\Pi^f_{\text{low}}\left(Q^2\right) = \sum_{j=1}^{M} g^{f2}_j \frac{m^{f2}_j}{m^{f2}_j + Q^2} + \sum_{j=0}^{N-1} a^f_j \left(Q^2\right)^j , \quad (11)$$

$$\Pi^f_{\text{high}}\left(Q^2\right) = \log\left(Q^2\right) \sum_{j=0}^{B-1} b^f_j \left(Q^2\right)^j + \sum_{j=0}^{C-1} c^f_j \left(Q^2\right)^j \quad (12)$$

and the full fit function is given by the sum of low- and high-momentum part weighted by Heaviside step functions

$$\Pi^f\left(Q^2\right) = \left(1 - \Theta\left(Q^2 - Q^2_{\text{match}}\right)\right) \Pi^f_{\text{low}}\left(Q^2\right) +$$
$$+ \Theta\left(Q^2 - Q^2_{\text{match}}\right) \Pi^f_{\text{high}}\left(Q^2\right) . \quad (13)$$

The set of pairs $\left\{\left(g^f_i, m^f_i\right) \mid i = 1, \dots, M\right\}$ of couplings and masses are determined from the corresponding connected, time-dependent single-quark-flavor vector current 2-point function at zero momentum. The remaining polynomial in Π_{low} can be understood as the contributions from poles with position above Q^2_{match}; for these terms we can safely use a Taylor expansion around the origin. We emphasize, that Π_{high} is only relevant for interpolation of the lattice data.

Finite volume effects related to the infrared momentum cut-off and the dependence on the specific fit function are then probed by varying the number of parameters M, N, B, C. In practice, we can resolve $M = 1$ or 2 poles with $N = 1, 2$ polynomial terms. Beyond that the fit parameters both from the multi-exponential fit of the vector current 2-point function as well as the fit of the vacuum polarization function become highly correlated. Moreover, the variation of B and C leads to insignificant variations of the integral value.

External scales problem and modified observables

As a peculiarity of the lattice QCD regularization, which excludes the dynamics of leptons and photons, the lepton mass in equation (2) enters as an external scale, which is not related to the lattice parameters. In particular, there is no inherent value for the lepton mass in lattice units, such that the lattice spacing is explicitly required to convert the lepton mass to lattice units. By this procedure, however, the originally dimensionless a^{hlo}_l becomes effectively dependent on the lattice QCD scale setting, which can be monitored by considering its effective dimension at fixed bare coupling [25, 26],

$$d_{\text{eff}}\left[a^{\text{hlo}}_l\right] = -\left(\frac{a}{a^{\text{hlo}}_l}\right)\left(\frac{\partial a^{\text{hlo}}_l}{\partial a}\right)\Bigg|_{g_0 = \text{fixed}} = O(-2 \sim -1)$$

The latter ranges from approximately -2 for the electron to -1 for the tau, such that a^{hlo}_l behaves rather like an inverse mass, $M^{d_{\text{eff}}}$, than a dimensionless quantity. This external scale problem has been solved by introducing a new family

of modified observables, $a^{\text{hlo}}_{\bar{l}}$ defined as follows. We denote with $\tilde{Q}$ the momentum in lattice units and can rewrite the integral in equation (2) in terms of $\tilde{Q}$ and define for any QCD scale H, which can be calculated on the lattice

$$a^{\text{hlo}}_{\bar{l}} = 4 \alpha^2 \int \frac{d\tilde{Q}^2}{\tilde{Q}^2} \Pi^{\gamma\gamma}_R\left(\tilde{Q}^2\right) w\left(\frac{\tilde{Q}^2}{a^2 H^2} \cdot \frac{H^2_{\text{phys}}}{m^2_l}\right) \quad (14)$$

with the consistency condition

$$\lim_{m_{PS} \to m_\pi} H(m_{PS}) = H_{\text{phys}}(m_\pi)$$

such that at the physical point the modified observable agrees with the standard definition for each choice of a consistent H

$$\lim_{m_{PS} \to m_\pi} a^{\text{hlo}}_{\bar{l}}(m_{PS}) = a^{\text{hlo}}_l(m_\pi) . \quad (15)$$

The introduction of a QCD-scale H redefines the lepton mass in the lattice calculation

$$m_{\bar{l}} = m_l/H_{\text{phys}} \cdot H ,$$

such that the modified lepton mass becomes dependent on the lattice scale setting and

$$d_{\text{eff}}\left[m^2_{\bar{l}}\right] = 2 \quad \text{and} \quad d_{\text{eff}}\left[a^{\text{hlo}}_{\bar{l}}\right] = 0 .$$

In practice we use the empirically motivated choice $H = m_V$, the mass of the ground state in the light vector channel. This exploits the strong statistical correlation of the light vector meson mass and a^{hlo}_l.

Extrapolation and results

To extrapolate in the light pseudoscalar mass to the physical point $m_{PS} \to m_\pi$ and to the continuum we use the ansatz

$$a^{\text{hlo}}_{\bar{l}}(m_{PS}, a) = A + B_1 m^2_{PS} \left(+B_2 m^4_{PS} + \dots\right) + C a^2 . \quad (16)$$

These extrapolations of the lattice data for $a^{\text{hlo}}_{\bar{l}}$ are shown in figure [5] for electron (top), muon (center) and tau lepton (bottom). Inspection by eye of the data points strongly suggests a linear dependence of the modified observable $a^{\text{hlo}}_{\bar{l}}$ on the pion mass and it turns out, that usually optimizing only B_1 already provides a good fit. With (at most) B_2 we probe for potential non-linearity in the pion mass dependence of our lattice data, which turns out to be insignificant. The three dashed lines in each plot show the evaluation of the fit function for the corresponding lattice spacing. The result for zero lattice spacing and physical pion mass is given by the red downward triangle shifted slightly off to the left from the physical pion mass marked by the vertical dashed line.

Additionally, in figure [6] we show the light-quark contribution (using only Π^{u+d}) for $a^{\text{hlo}}_{\bar{l}}$ for all three leptons: we compare the results from the $N_f = 2+1+1$ simulations, which are extrapolated to the physical pion mass ([18, 19]) with the recent calculation on an ETMC $N_f = 2$ ensemble
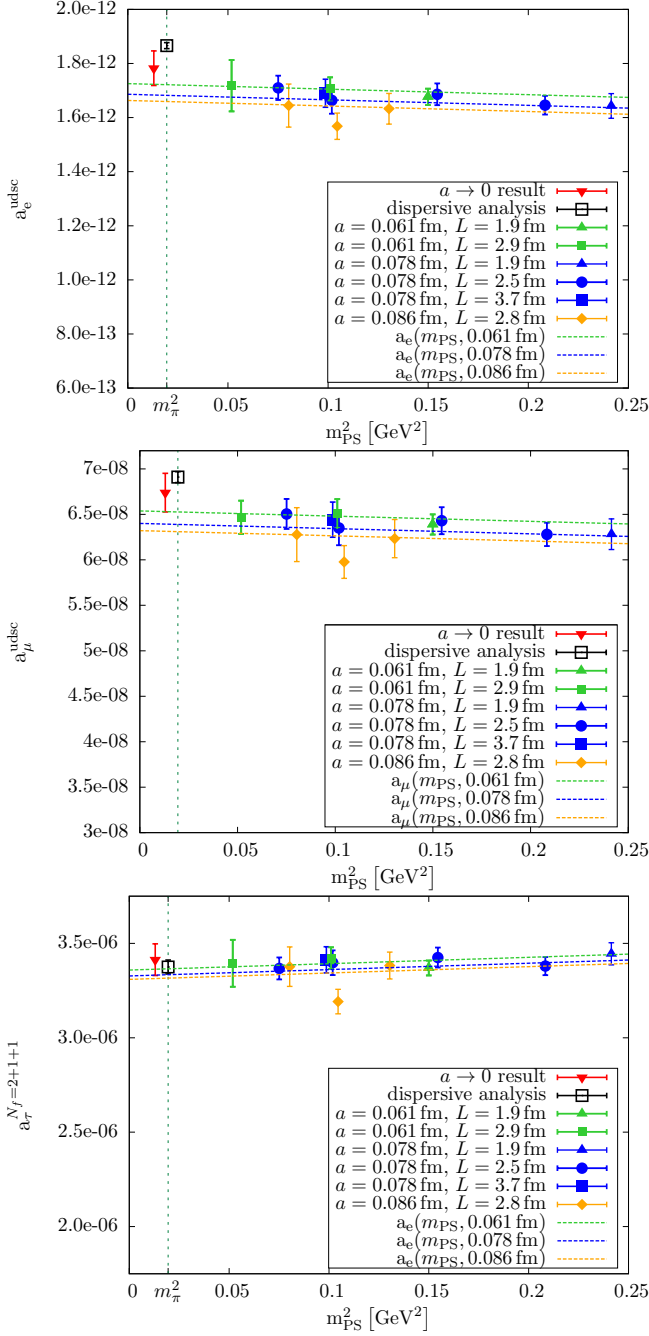
Figure 6. Light-quark contribution to a_l^{hlo} at physical pion mass for electron (top), muon (center) and tau (bottom) from the standard definition with $H = 1$ (cf. eq. (14)); shown is the comparison of the m_{PS}^2- extrapolated data from [18, 19] with the result calculated directly at the physical pion mass [21].

Systematic uncertainties and error budget

We investigate comprehensively the impact of all systematic uncertainties X in our lattice calculation and call the corresponding estimate Δ_X. In detail we probe

(i) finite size effects, Δ_{FSE}, by restricting the range in $m_{PS} \cdot L$ of lattice data entering the combined continuum and chiral extrapolation to $m_{PS} \cdot L > 3.8$ and by comparing a_l^{hlo} for ensembles with different lattice volumes at fixed lattice spacing and pion mass;

(ii) the impact of data from larger pion masses, Δ_χ, by restricting to lattice data in the range $m_{PS} < 400\,\text{MeV}$;

(iii) the impact Δ_V of varying the fit range for the vector meson 2-point function;

(iv) the dependence on the fit function Δ_{MNBC} by varying the number of parameters M, N, B, C (cf. eq. (11), (12));

(v) the impact of disconnected contributions, Δ_{disc};

(vi - viii) the uncertainty from matching the Osterwalder-Seiler quark masses, Δ_{OS}, from varying the transition point from low- to high-momentum region, $\Delta_{Q_{\text{match}}^2}$, and the uncertainty from mistuned strange and charm sea quark masses, $\Delta_{(\mu_\sigma, \mu_\delta)}$.

Though some of these effects are likely correlated, in particular (i) and (iv), we take a conservative approach and check each uncertainty individually, thus potentially overestimating the overall uncertainty. As a general observation, the contributions from (vi) to (viii) are negligible and we set $\Delta_{\text{OS}} = \Delta_{Q_{\text{match}}^2} = \Delta_{(\mu_\epsilon, \mu_\delta)} = 0$. For (v) we showed above (cf. figure [3]), that with presently available statistics, the impact of disconnected contributions is also negligible in our calculation, they do not lead to a statistically significant shift of the result. Moreover, the lattice data

Figure 5. Combined extrapolation in pion mass and lattice spacing for $a_{\bar{l}}^{\text{hlo}}$ for electron (top), muon (center) and tau (bottom) using free fit parameters A, B_1, C in equation (16).

directly at physical pion mass [21]. The results for the simulation directly at the physical pion mass are obtained using the standard definition of the observables (cf. eq. (2) or (14) with $H = 1$). Within presently reachable statistical uncertainties, there is full agreement of extrapolated results and results obtained from the simulation at physical pion mass.
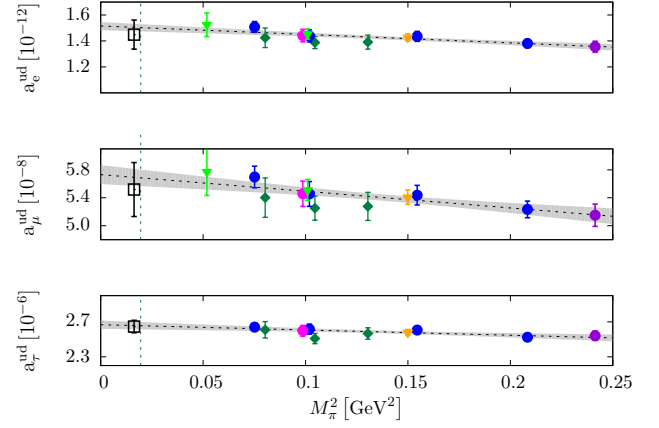
Table 2. Estimates for systematic uncertainties Δ_V and Δ_{MNBC} for our lattice calculation.

a_l^{hlo}	Δ_V	Δ_{MNBC}
e	$0.035 \cdot 10^{-12}$	$0.078 \cdot 10^{-12}$
μ	$0.13 \cdot 10^{-8}$	$0.09 \cdot 10^{-8}$
τ	$0.046 \cdot 10^{-6}$	$0.032 \cdot 10^{-6}$

Table 3. Comparison of results for a_l^{hlo} from $N_f = 2 + 1 + 1$ lattice QCD (center) and dispersive analyses (right).

a_l^{hlo}	tmLQCD	disp. analyses
e	$1.782\,(64)\,(85) \cdot 10^{-12}$ [18]	$1.866\,(10)\,(05) \cdot 10^{-12}$ [13]
μ	$6.78\,(24)\,(16) \cdot 10^{-8}$ [19]	$6.91\,(01)\,(05) \cdot 10^{-8}$ [14]
τ	$3.41\,(8)\,(6) \cdot 10^{-6}$ [18]	$3.38\,(4) \cdot 10^{-6}$ [15]

for a_l^{hlo} in figure [5] covering $3 \lesssim m_{PS} \cdot L \lesssim 6$ and the extrapolations indicate small finite size effects, which is confirmed again by the statistical analysis. Already above we commented on the apparently highly dominant linear dependence of the modified a_l^{hlo} on the m_{PS}^2. This too leads to statistically non-discernible effects when probing for terms of higher than first order in m_{PS}^2 with the present data. We list the estimates for the remaining two sources of systematic errors in table {2}. Finally, in table {3} we list the complete results for a_l^{hlo} for electron, muon and tau and compare to the results from phenomenological analyses based on dispersion relations and using experimental data. Where available, we give the decomposition of the total error $(\Delta_{\text{stat}})\,(\Delta_{\text{sys}})$ into statistical uncertainty in the first bracket and the second bracket quotes the systematic uncertainty. The systematic uncertainty for the lattice results is obtained as $\Delta_{\text{sys}} = \sqrt{\sum_X \Delta_X^2}$.

3 Discussion and outlook

With this contribution we report on the determination of the hadronic leading order anomalous magnetic moments of all three Standard Model leptons by the ETM Collaboration with $N_f = 2 + 1 + 1$ dynamical quarks. The center column of table {3} gives our estimates for a_l^{hlo} in the continuum and at the physical pion mass with statistical and a conservatively determined overall systematic uncertainty. We find agreement with the estimates from phenomenological analyses within presently reached uncertainties. With the lattice data available for this analysis the uncertainties from the lattice calculation are still significantly larger than those obtained from the dispersive analyses. As a result of this analysis we reach a precision of roughly 6% and 4% for the case of the electron and muon, respectively, and of 3% for the tau lepton with combined statistical and systematic error. The smaller uncertainty for the case of the tau may be expected, since the main support for the integral in equation (2) is shifted towards a region of momenta, where lattice data for the vacuum polarization tensor is actually available. Yet we emphasize, that also in this case there is a critical dependence

on the extrapolation of the vacuum polarization function in the small-momentum region: it appears through the subtraction of $\Pi^{\gamma\gamma}(Q^2 = 0)$, and this latter value is predicted from the extrapolation of the lattice data. The determination of a_e^{hlo} on the lattice is a strong test of the lattice determination of the vacuum polarization function at smallest momenta, since a_e^{hlo} is essentially determined by the derivative of the polarization function at the origin, $d\Pi^{\gamma\gamma}(Q^2)/dQ^2\big|_{Q^2=0}$. Thus the agreement obtained for a_e^{hlo} is both remarkable and encouraging. With the results from our recent determination of the hadronic leading order contribution to the running of the electroweak couplings [27], this test has been successfully taken another step further: in this reference we demonstrate the agreement of the renormalized vacuum polarization function determined from $N_f = 2 + 1 + 1$ twisted mass lattice QCD with the dispersive relation result in a continuous interval $\left[0, 10\,\text{GeV}^2\right]$, albeit again with somewhat larger uncertainty on the lattice result.

The use of the modified observables a_l^{hlo} (cf. equation (14)) at unphysically large pion masses and non-zero lattice spacing has proven superior to the standard definition of a_l^{hlo} in equation (2) in our lattice calculation. The reason is twofold: Firstly, it is due to the introduction of the scale H, that the strong pion mass dependence of a_l^{hlo} is tamed to the level shown in figure [5]. As a result we are able to perform a controlled chiral extrapolation with insignificant variations of the result when probing the pion mass dependence beyond the leading, linear term. With the standard definition a controlled extrapolation from the range of pion masses we have available (cf. table {1}) will require some modeling or otherwise lead to a prohibitively large uncertainty at the physical point (cf. [25, 26] for a more detailed discussion). Secondly, by an optimized choice of the scale H, which for us is $H = m_V$, the light vector meson mass, the per-ensemble estimate of a_l^{hlo} benefits from a partial cancellation of statistical errors due to the correlation of the vector meson mass and coupling and the polarization function. Both advantageous features of this mechanism have been put to work in [27] as well with the above described positive outcome. Moreover, the direct comparison of the light-quark contribution from extrapolation in $m_{PS}^2 \to m_\pi^2$ and direct calculation at the physical pion mass, which is done without any modification of the observable, provides further confirmation of the present results' consistency, but this test has to be made more stringent by achieving higher statistical accuracy for the result from direct simulation at the physical pion mass.

The more accurate ab-initio determination of a_l^{hlo} directly at the physical pion mass is an on-going effort within the ETMC. The evaluation of the crucial light quark contribution for $N_f = 2$ dynamical fermions at physical pion mass along the lines of [21] for a larger volume with $m_{PS} \cdot L = 4$ is on-going. Moreover, with the continuing simulation activity of the ETMC aiming for gauge field ensembles with fully dynamical up, down, strange and charm quark with physical values for the pion, Kaon and D-meson mass we have for the near future the prospect of calculating a_l^{hlo} in a setup including QCD-dynamics from

the first two families of quark flavors with quark masses at their physical values.

We are then basically left with the systematic effect of the finite volume in the form of the infrared cut-off $\sim 1/L$ of the lattice data. Lattice simulations in larger physical volumes are an essential yet at present computationally cost-intensive way to constrain further the polarization function at smallest momenta. Beyond that alternative methods have been proposed and are being developed (e.g. [30–32]) to exploit further the analytic structure of the polarization function in finite volume to constrain its shape in the small momentum region.

References

[1] T. Blum, Phys. Rev. Lett. **91** (2003) 052001 [hep-lat/0212018].

[2] G. F. Giudice, P. Paradisi and M. Passera, JHEP **1211** (2012) 113 [arXiv:1208.6583 [hep-ph]].

[3] N. Brambilla *et al.*, Eur. Phys. J. C **74** (2014) 10, 2981 [arXiv:1404.3723 [hep-ph]].

[4] M. Fael, L. Mercolli and M. Passera, Nucl. Phys. Proc. Suppl. **253-255** (2014) 103 [arXiv:1301.5302 [hep-ph]].

[5] B. Oberhof [BaBar Collaboration], Nucl. Part. Phys. Proc. **260** (2015) 12 [arXiv:1502.01810 [hep-ex]].

[6] R. Baron *et al.*, JHEP **1006** (2010) 111 [arXiv:1004.5284 [hep-lat]].

[7] R. Baron *et al.* [European Twisted Mass Collaboration], Comput. Phys. Commun. **182** (2011) 299 [arXiv:1005.2042 [hep-lat]].

[8] K. Osterwalder and E. Seiler, Annals Phys. **110** (1978) 440.

[9] R. Frezzotti and G. C. Rossi, JHEP **0408** (2004) 007 [hep-lat/0306014].

[10] R. Frezzotti and G. C. Rossi, JHEP **0410** (2004) 070 [hep-lat/0407002].

[11] C. Aubin, T. Blum, M. Golterman and S. Peris, Phys. Rev. D **86** (2012) 054509 [arXiv:1205.3695 [hep-lat]].

[12] F. Jegerlehner, Nucl. Phys. Proc. Suppl. **181-182** (2008) 26.

[13] D. Nomura and T. Teubner, Nucl. Phys. B **867** (2013) 236 [arXiv:1208.4194 [hep-ph]].

[14] F. Jegerlehner and R. Szafron, Eur. Phys. J. C **71** (2011) 1632 [arXiv:1101.2872 [hep-ph]].

[15] S. Eidelman and M. Passera, Mod. Phys. Lett. A **22** (2007) 159 [hep-ph/0701260].

[16] A. Abdel-Rehim *et al.*, PoS LATTICE **2013** (2014) 264 [arXiv:1311.4522 [hep-lat]].

[17] A. Abdel-Rehim *et al.*, PoS LATTICE **2014** (2015) 119 [arXiv:1411.6842 [hep-lat]].

[18] F. Burger, G. Hotzel, K. Jansen and M. Petschlies, arXiv:1501.05110 [hep-lat].

[19] F. Burger *et al.* [ETM Collaboration], JHEP **1402** (2014) 099 [arXiv:1308.4327 [hep-lat]].

[20] F. Burger, G. Hotzel, K. Jansen and M. Petschlies, JHEP **1503** (2015) 073 [arXiv:1412.0546 [hep-lat]].

[21] A. Abdel-Rehim *et al.* [ETM Collaboration], arXiv:1507.05068 [hep-lat].

[22] Y. Iwasaki, Nucl. Phys. B **258** (1985) 141.

[23] M. Golterman, K. Maltman and S. Peris, Phys. Rev. D **90** (2014) 7, 074508 [arXiv:1405.2389 [hep-lat]].

[24] M. Golterman, K. Maltman and S. Peris, Phys. Rev. D **88** (2013) 11, 114508 [arXiv:1309.2153 [hep-lat]].

[25] D. B. Renner, X. Feng, K. Jansen and M. Petschlies, PoS LATTICE **2011** (2012) 022 [arXiv:1206.3113 [hep-lat]].

[26] X. Feng, K. Jansen, M. Petschlies and D. B. Renner, Phys. Rev. Lett. **107** (2011) 081802 [arXiv:1103.4818 [hep-lat]].

[27] F. Burger, K. Jansen, M. Petschlies and G. Pientka, arXiv:1505.03283 [hep-lat].

[28] F. Jegerlehner, Nuovo Cim. C **034S1** (2011) 31 [arXiv:1107.4683 [hep-ph]].

[29] C. Michael *et al.* [ETM Collaboration], Phys. Rev. Lett. **111** (2013) 18, 181602 [arXiv:1310.1207 [hep-lat]].

[30] D. Bernecker and H. B. Meyer, Eur. Phys. J. A **47** (2011) 148 [arXiv:1107.4388 [hep-lat]].

[31] X. Feng, S. Hashimoto, G. Hotzel, K. Jansen, M. Petschlies and D. B. Renner, Phys. Rev. D **88** (2013) 034505 [arXiv:1305.5878 [hep-lat]].

[32] B. Chakraborty, C. Davies, P. Gonçalves de Oliveira, J. Koponen, G. P. Lepage, PoS LATTICE **2015** (2015) Talk given at the 33rd International Symposium on Lattice Field Theory, Kobe, Japan, 2015.